Simulation of the solute transport and microstructure evolution during the selective laser melting process

Simulation of the solute transport and microstructure evolution during the selective laser melting process

Neng Ren[1], Jun Li[1,*], Chinnapat Panwisawas[2], Mingxu Xia[1], Hongbiao Dong[3], Jianguo Li[1]

1. Shanghai Key Laboratory of Advanced High-temperature Materials and Precision Forming, School of Material Science and Engineering, Shanghai Jiao Tong University, Shanghai 200240 P.R. China

2. School of Engineering and Materials Science, Queen Mary University of London, London E1 4NS, United Kingdom

3. School of Engineering, University of Leicester, Leicester LE1 7RH, United Kingdom

E-mail: li.jun@sjtu.edu.cn (Jun Li)

Abstract. Selective laser melting is of great expectation to be used in additive manufacturing of aerospace components with complex geometry. However, there are still defects in the built parts, such as solutal segregation and unexpected microstructure, which contribute to cracks and lead to failure. At present, most of the simulations focus on the macroscopic grain structure, and the solute transport process has not been well demonstrated yet. In the present work, we develop a two-way fully coupled model based on cellular automaton and finite volume method to simulate the solute transport and dendritic structure evolution during the melting and solidification of the SLM process. The results reveal the microstructural evolution and solute transport during the melting, spreading, and smearing of the powder. The proposed model framework shows good potential to be applied to further numerical investigation on the solidification behaviours of the SLM process.

1. Introduction

In aerospace and medical fields, selective laser melting (SLM) is one of the most promising additive manufacturing methods for the precision forming of the components [1]. However, this developing technique still faces problems in providing parts of reliable working performance, such as the cracks in the built superalloys[2]. Grain structure and solute segregation are generally considered to be factors determining the crack susceptibility, and should be further understood and strictly controlled. Due to the difficulties in the in-situ observation of superalloys, numerical simulation is an important choice to study the cycled melting and solidification of the SLM process.

Recent decades, multi-scale models have been developed [3] and then applied to understand the grain structure of the built parts. Lian et al.[4], developed a parallelized 3D cellular automaton computational model to predict grain morphology for solidification of metal during the additive manufacturing process, where a one-way coupling strategy is used to account the temperature field. Yang et al.[5] established a

phase field- thermal fluid flow model to simulate grain evolutions during powder-bed-fusion. Especially, the solid-state grain coarsening in the heat affected zone was reproduced. However, rather a few numerical simulations have taken the effect of melt convection on the solute transport into account. Shinjo et al.[6] demonstrated the solute transport of common solute elements in the metal pool on the macroscopic scale via computational fluid dynamics (CFD) simulations, but the solute distribution is not coupled with grain structure. Although Yu et al.[7] made attempts to evaluate the impact of fluid flow on the dendritic growth and the formation of new grain in additive manufacturing, their simulation is actually based on the pre-defined flow field. For the grain structure prediction, up till now, what most of the simulations focused on is the grain structure, but the solute distribution, including but not limited to the solute enrichment in the grain boundaries and interdendritic regions, was not well demonstrated. In the hard-to-print alloy systems, such as superalloys, the solute element distribution is also of great importance to estimate the crack susceptibility.

In this paper, based on cellular automaton and finite volume method, we develop a two-way fully coupled model to simulate the solute transport and dendritic structure evolution during the melting and solidification of the SLM process. Necessarily, the two-phase flow of gas and liquid metal as well as heat transfer are also included in the model framework. Except for the thermal-fluid dynamic aspects as well as the concomitant solute transport of the SLM process, the fusion of the powder and substrate, liquation of the interdendritic region, and the melting of the dendritic trunks are also well demonstrated. Thus, the proposed model framework provides a powerful tool to study the solutal segregation and alloying process in the SLM and the other additive manufacturing process.

2. Model description

Based on the combined cellular automaton and finite volume method, we develop a fully-coupled model describing the multi-physical fields (including temperature field, flow field, and solute element field) and evolution of dendritic structure on the same set of computational grids. The control volumes in finite volume framework are also employed as the cells in cellular automaton, and hence the multiple physics are two-way fully coupled with dendritic structure.

2.1. Multiphase flow

Generally, there are three phases considered in the CFD simulation of SLM process, liquid melt (fused substrate and powder), gas (air or protective gas such as argon), solid metal (including unfused substrate and powder, and solidified melt). In our model framework, we did not distinguish the liquid melt and solid metal as two separated fluid phases. Instead, we use solid volume fraction to characterize the local solidification or melting sequence. Considering the significant change in the surface morphology of the powder during the melting process, volume of fluid approach is used to track the interface due to its powerful robustness in handling two-phase interface. The continuity equation is as follows:

$$\frac{\partial \alpha}{\partial t} + (\vec{v} \cdot \nabla)\alpha = 0 \tag{1}$$

where α is the volume fraction of gas or metal, vector $\boldsymbol{v}$ is the velocity of fluid, t is time. Consequently, the physical properties in each control volume, such as viscosity and thermal physical properties, are the volume averaged ones of the two phases under the finite volume model framework. It should be noted that the sum of the volume fractions of gas and metal is unity.

Navier-Stokes equations is used to describe the fluid flow in the SLM process. The fluid of gas and metal is assumed to be incompressible, and the density dependence on the temperature and solute concentration is described using Bousinesq approximation, where the density difference is regarded as body forces in the momentum conservation.

$$\left[\frac{\partial\left(\rho\vec{v}\right)}{\partial t} + \nabla\cdot\left(\rho\vec{v}\vec{v}\right)\right] = -\nabla p + \nabla\cdot\left(\mu\nabla\vec{v}\right) + \vec{F}_T + \vec{F}_C + \vec{F}_M + \vec{F}_{st} \tag{2}$$

where ρ is density, μ is dynamic viscosity, p is pressure, and the four sources stand for thermal buoyancy, solutal buoyancy, momentum damp in mushy zone, and surface tension, respectively. Thermal

expansion coefficient and solutal expansion coefficient are used to cover the deviation from the density under reference temperature and nominal composition. The momentum damp in the solid/liquid interface is described with Blake-Kozeny equation, where the resistance is the function of solid volume fraction. Surface tension is calculated using the continuum surface force model, and Marangoni effect is described with temperature dependent surface tension coefficient [8].

2.2. Heat transfer

Enthalpy equation is used to calculate the heat transfer during the SLM process, where enthalpy equals to the temperature integral of specific heat. Latent heat released during solidification or absorbed during melting is loaded as a source term. The latent heat absorbed by evaporated metal is similar, but the phase of metal vapor is neglected in the continuity and momentum equations. Besides, the thermal boundary conditions on the gas/metal interfaces are also loaded as source terms using the interfacial operator under the volume of fluid framework.

$$\frac{\partial \rho \vec{v} h}{\partial t} + \nabla \cdot (\rho \vec{v} h) = \nabla \cdot (\lambda \nabla T) + Q \tag{3}$$

where h is sensible enthalpy, λ is thermal conductivity, T is temperature, and Q is the heat sources, including latent heat of fusion and evaporation, convective and radiative gas/metal interfacial thermal dissipation, and laser power input [9].

2.3. Species transport

Two sets of solute conservation equations are employed for the solute elements in liquid melt and solidified metal. In the melt, except for the solutal diffusion and the species transfer caused by melting or solutal partition during solidification, the solute transport induced by melt convection is also included[10]. The species transfer caused by the solid-liquid transition is loaded as source terms in the two equations.

$$\frac{\partial \alpha_m \rho_m C_l}{\partial t} + \nabla \cdot (\alpha_m \rho_m \vec{v} C_l) = \nabla \cdot (D_l \alpha_m \rho_m \nabla C_l) + C_{ml} \tag{4}$$

$$\frac{\partial \alpha_m f_s C_s}{\partial t} = \nabla \cdot (D_s \alpha_m \rho_m f_s \nabla C_s) + C_{ms} \tag{5}$$

where C is the mass fraction of certain solute element, D is solute diffusivity, C_{ml} and C_{ms} are solutal sources induced by phase transformation, f_s is solid volume fraction, and the subscript l and s represent liquid and solid, respectively.

2.4. Dendritic evolution

Cellular automaton method is used to describe the preference growth of the dendritic structure. Two states of active and inactive are defined to govern the dendritic structural evolution. Active state means phase transformation as well as the concomitant heat and mass transfer would occur in the local control volume, while they are impossible to occur in the control volumes of inactive state. In other words, the inactive state means steady liquid or solid phase. Von-Neumann neighbour is used in the cellular automaton framework for the moment, and neighbour control volumes are captured by the active one when the dendritic tip touches their borders.

Except for being captured by active control volume, the inactive control volume is activated when the local undercooling reaches the critical nucleation undercooling, or the local temperature increases to the eutectic temperature. Conversely, the active state is converted to inactive when the local solid volume fraction decreases to zero, or the temperature drops under the eutectic temperature. It should be noted that only in the control volume whose metal volume fraction is larger than 0.5 can the inactive control volume be converted to the active state. Thermodynamical equilibrium condition is used to calculate the melting or solidification progressing[11], i.e., the solid volume fraction change:

$$\Delta f_s = f_l \frac{C_l^* - C_l}{C_l^*(1-k)} \tag{6}$$

where k is partition coefficient, f_l is liquid volume fraction, and the superscript * represent the equilibrium condition. It should be noted that the solid volume fraction here ranges from zero to unity, and the product of f_s and the volume fraction of metal α_m is the actual solid volume fraction of the control volume.

2.5. Simulation parameters

The SLM process of IN 718 is simulated, and the operating parameters and material properties are listed in Table 1. According to it is reported by Lee et al.[12], for the metal pool of SLM, such as SLM-ed nickel-based superalloy IN 718, the scale along the scanning direction (about 750 μm) is much longer than the scale perpendicular to the scanning path (180 μm or so). Therefore, though SLM process is actually three-dimensional for strictly speaking, it could still be sensible to perform two-dimensional simulation to capture certain characteristic of the multi-physical field transports in the process.

Figure 1 shows the computational domain and schematic diagram of laser heat source on the surface of the powder. The two-dimensional computational domain is the longitudinal section perpendicular to the scanning path, and the heat flux is calculated according to the section of the three-dimensional Gaussian distribution profile. The complicated reflection in the powder layer is simplified to be uniformly distributed on the gas/metal interfaces of both the powder and the substrate.

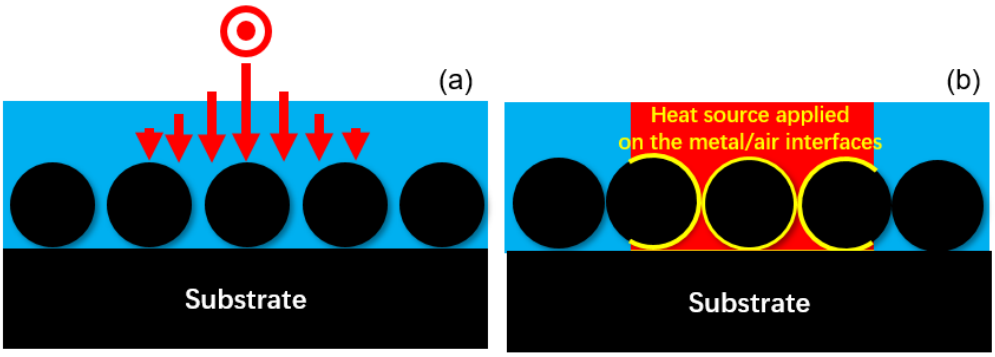

Figure 1. Schematic diagram of heat source induced by laser input in SLM.

Table 1. Processing parameters and material properties.

Parameters	Value
Laser scanning speed, m/s	0.96
Laser power, W	50
Diameter of laser beam spot, μm	100
Diameter of powder, μm	15
Convective heat transfer coefficient, W/m^2-K	80
Property	
Liquidus temperature, K	1609
Solidus temperature, K	1523
Surface tension coefficient, kg/s^2	1.882
Temperature coefficient of surface tension, kg/s^2-K	-1E-4

According to the reported solutal partition coefficients of the solute elements in the IN 718, Nb shows the most severe segregation tendency. Considering the great challenges in describing the solidification path and dynamical process in the multicomponent superalloys in numerical modelling, based on the assumption that the interactions of alloy elements on the solidification path could be neglected, only the Ni-Nb binary system in the superalloy IN 718 is focused on in the benchmark simulation case. The phase

diagram parameters are listed in Table 2. For the stability of the solution process, the binary system is further linearised using constant partition coefficient and slope of liquidus.

Table 2. Phase-diagram parameters of the Ni-Nb binary system in IN 718

Parameters	Value
Partition coefficient	0.48
Slope of liquidus, K wt.$^{-1}$	-10.50
Critical nucleation undercooling degree, K	9.2
Standard deviation of Gaussian distribution, K	2.0
Maximum of nucleation density, m^{-3}	10^{10}
Solutal diffusion coefficient in liquid, m/s^2	2E-9

3. Results and discussion

Figure 2 shows the melting process of the powder and the substrate, as well as the liquation of the interdendritic region of the substrate. The grey scale in the left half of the contour stands for the mass fraction of solute elements, and the isolines coloured in rainbow colour map is isotherms. On the right half of the contour, rainbow colour map represents the local solid volume fraction, which indicates the sequence of melting and solidification, while red arrows are velocity vectors. The initial condition of the benchmark case of the SLM process is shown in Figure 1a, where the solute element is diluted in the dendritic trunks while enriched in the interdendritic region.

As the laser heat source is applied to the surface of the powder, the heat transfers from the surface to centre quite fast, and metal droplets are formed before the melt flows downward to the surface of the substrate. The interdendritic region is liquated first, that is the low melting point eutectic phases considered in our model framework. Actually, other phases of low melting point, such as Lave phases, carbides, and even borides in some kinds of superalloys, are also formed and growing in the interdendritic regions.

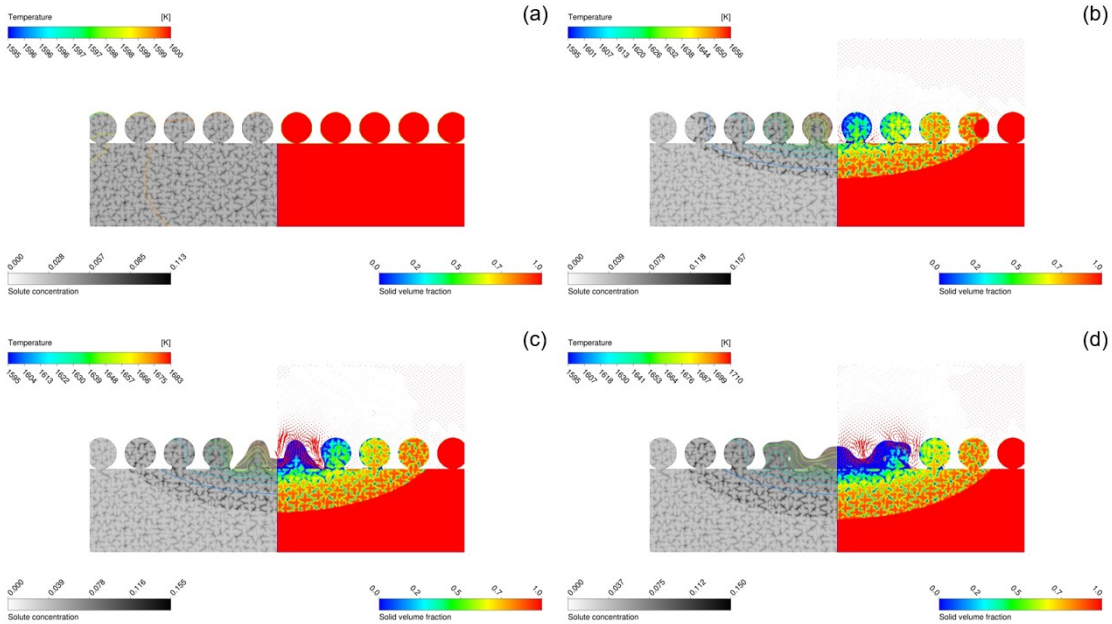

Figure 2. Melting of the powder and liquation of the interdendritic region in the substrate.

Figure 3 demonstrate the spreading and smearing of the fused powder. The metal droplets collapse, and the melt/gas interface spreads laterally. The spreading of the metal droplets and the fusion of the

substrate leads to the formation of a shallow metal pool. The periphery powder is smeared by the free surface of the metal pool, and then heated to be fused. As soon as the part of the powder is fused, the local solute distribution is significantly changed under the melt convection. The enriched solute in the interdendritic region and dilute solute in the original dendritic trunks are well mixed, and thus there is an obvious boundary between the solute uniformly distributed metal pool and solute segregated powder and substrate.

In the heat affected zone, though the dendritic trunks are not completely remelted, the interdendritic region has already completely liquated. Therefore, the dendritic trunks are actually loosely connected with each other in the liquid films. Although the melt convection in the metal pool is rather intensive, the interdendritic flow is still rather weak and hardly influenced by the fully-fused bulk region. Consequently, the solute originally enriched in the interdendritic region could not be transferred away by convection. It can be deduced that the liquation in the heat affected zone would not lead to the change in the local composition. Furthermore, under a relatively lower temperature, the liquid film among the dendritic trunks suffers smaller thermal stress during the thermal cycles, and hence the risk of hot tearing could be much smaller.

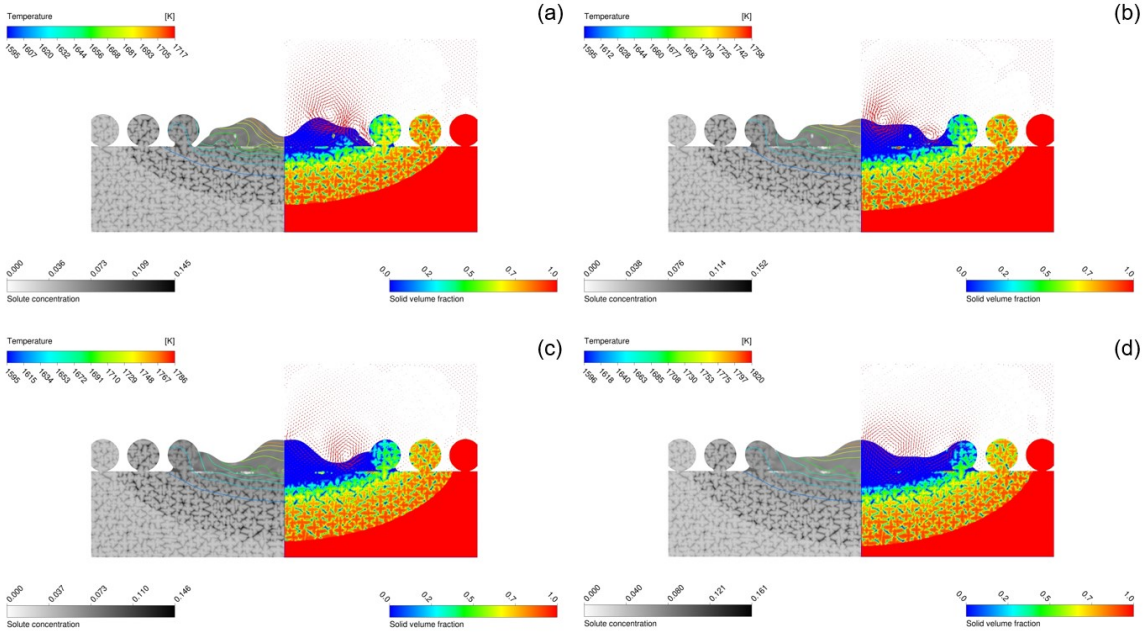

Figure 3. Spreading and smearing of the melted powder.

Figure 4 shows the oscillation of the free surface and the induced convection-driven solute transport in the metal pool. It should be noted that the temperature of the liquid metal does not reach the boiling temperature, and thus there is no recoil pressure acting on the free surface of the metal pool. Therefore, the metal pool is much shallower than the keyhole-mode SLM process, and consequently the melt flow is much weaker. Without the effect of the recoil pressure, the spreading and oscillating of the free-surface plays the dominating role in the expanding of the metal pool along both the horizontal and the building directions.

Besides, though the energy input is much smaller, a good metallurgical bonding still seems to be achieved between the fused powder and the substrate. However, the results need to be confirmed further in the actual powder layer of complicated particle distribution, where the fusion process shows more aspects, such as the lack of fusion, insufficient spreading of the free surface, and unexpected solidification of the border of the metal pool.

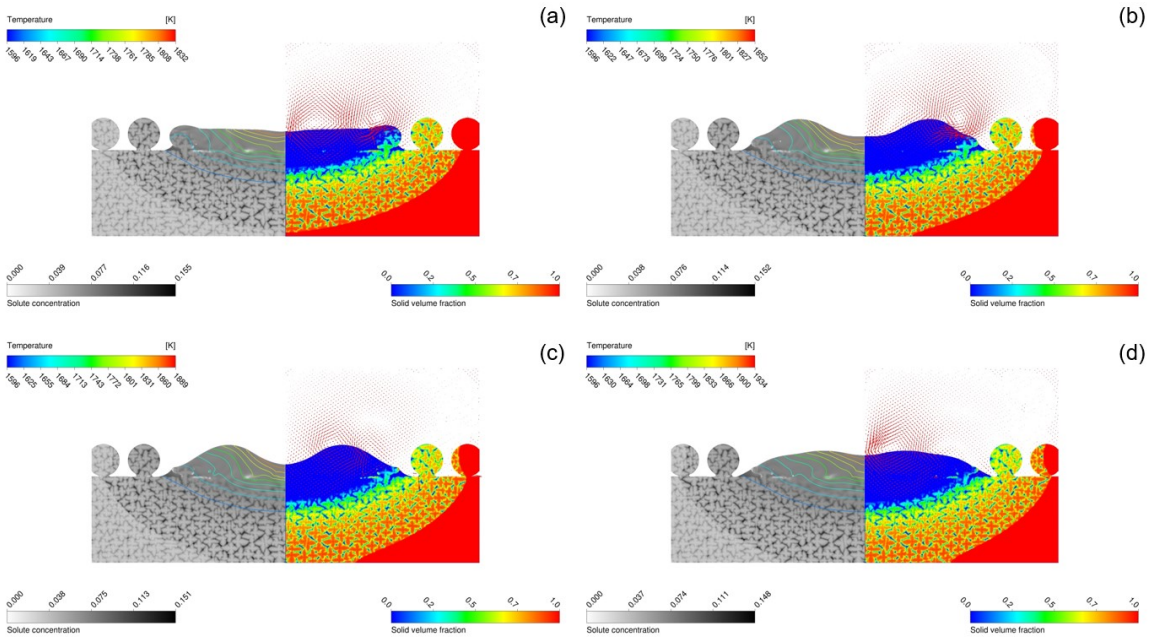

Figure 4. Oscillation of the gas/melt interface and solute transport in the metal pool.

4. Conclusions and perspective

A two-way fully coupled cellular automaton-finite volume model is developed to simulate the solute transport and dendritic structure evolution during the SLM process. The simulation results reveal the liquation in the interdendritic region, the fusion of dendritic trunks, and concomitant solute transport during the melting, spreading, and smearing of the powder. Under a relatively low heat input, when the peak of the temperature of the free-surface can not reach the boiling temperature, the free-surface dynamics plays the dominating role in the convection-driven solute mixing, and a good metallurgical bonding can still be achieved under this operating condition.

The presented model shows potential in predicting the solute transport on the scale of 10^{-7}~10^{-6} μm. The dendritic growth after the laser spot pass away is also expected to be demonstrated using the developed model in the further simulations. Besides, as it was discussed by Pinomaa et al.[13], the effect of rapid solidification can also be describe using the continuous growth model proposed by Aziz et al[14]. The local non-equilibrium solidification could be revealed by implicit solving the crystal growing rate, partition coefficient, and slope of liquidus.

Acknowledgements

This work was sponsored by National Natural Science Foundation of China (No. 52074182) and General fund of Shanghai Municipal Commission of science and technology (Grant No. 22ZR1430700).

References

[1] Panwisawas C, Tang Y T and Reed R C 2020 Metal 3D printing as a disruptive technology for superalloys *Nat. Commun.* **11** 2327

[2] Tang Y T, Panwisawas C, Ghoussoub J N, Gong Y, Clark J W G, Németh A A N, McCartney D G and Reed R C 2021 Alloys-by-design: Application to new superalloys for additive manufacturing *Acta Mater.* **202** 417–36

[3] Li J, Xu X, Ren N, Xia M and Li J 2022 A review on prediction of casting defects in steel ingots: from macrosegregation to multi-defect model *J. Iron Steel Res. Int.* **29** 1901–14

[4] Lian Y, Lin S, Yan W, Liu W K and Wagner G J 2018 A parallelized three-dimensional cellular automaton model for grain growth during additive manufacturing *Comput. Mech.* **61** 543–58
[5] Yang M, Wang L and Yan W 2021 Phase-field modeling of grain evolutions in additive manufacturing from nucleation, growth, to coarsening *npj Comput. Mater.* **7** 56
[6] Shinjo J and Panwisawas C 2021 Digital materials design by thermal-fluid science for multi-metal additive manufacturing *Acta Mater.* **210** 116825
[7] Yu Y, Wang L, Zhou J, Li H, Li Y, Yan W and Lin F 2022 Impact of fluid flow on the dendrite growth and the formation of new grains in additive manufacturing *Addit. Manuf.* **55** 102832
[8] Wang L and Yan W 2021 Thermoelectric Magnetohydrodynamic Model for Laser-Based Metal Additive Manufacturing *Phys. Rev. Appl.* **15** 64051
[9] Tang C, Tan J L and Wong C H 2018 A numerical investigation on the physical mechanisms of single track defects in selective laser melting *Int. J. Heat Mass Transf.* **126** 957–68
[10] Ren N, Li J, Panwisawas C, Xia M, Dong H and Li J 2021 Thermal-solutal-fluid flow of channel segregation during directional solidification of single-crystal nickel-based superalloys *Acta Mater.* **206** 116620
[11] Zhu M F and Stefanescu D M 2007 Virtual front tracking model for the quantitative modeling of dendritic growth in solidification of alloys *Acta Mater.* **55** 1741–55
[12] Lee Y S and Zhang W 2016 Modeling of heat transfer, fluid flow and solidification microstructure of nickel-base superalloy fabricated by laser powder bed fusion *Addit. Manuf.* **12** 178–88
[13] Pinomaa T, Lindroos M, Walbrühl M, Provatas N and Laukkanen A 2020 The significance of spatial length scales and solute segregation in strengthening rapid solidification microstructures of 316L stainless steel *Acta Mater.* **184** 1–16
[14] Aziz M J 1982 Model for solute redistribution during rapid solidification *J. Appl. Phys.* **53** 1158–68